

Enhanced electron-magnon scattering in ferromagnetic thin films and the breakdown of the Mott two-current model

R. M. Rowan-Robinson, A. T. Hindmarch, and D. Atkinson*

Department of Physics, Durham University, Durham DH1 3LE, United Kingdom

(Received 3 February 2014; published 2 September 2014)

Electron-magnon spin-flip scattering in thin films was studied by investigating the thickness dependence of the anisotropic magnetoresistance (AMR) effect and spin-wave stiffness. The absolute resistivity change due to the AMR effect ($\Delta\rho$) in Ni, Ni:V, and Ni:Cr doped films reduced with film thickness. This loss of AMR is due to enhanced spin-flip scattering, dropping at the same thickness irrespective of dopant. The spin-wave stiffness reduced at the same thickness, confirming enhanced electron-magnon spin-flip scattering. The AMR ratio was fitted with a simple model, in which thickness dependence was included in a spin mixing resistivity term. This analysis gives insight into the fundamental contribution of magnon scattering to the resistivity in thin films, which ultimately has relevance to spin coherence in spintronic devices.

DOI: [10.1103/PhysRevB.90.104401](https://doi.org/10.1103/PhysRevB.90.104401)

PACS number(s): 72.25.Mk, 75.30.Ds, 75.50.Cc, 75.76.+j

I. INTRODUCTION

The Mermin-Wagner theory applied to an ideal two-dimensional isotropic ferromagnet predicts spin fluctuations so strong that ferromagnetic order cannot exist [1]. In reality the anisotropy fields contribute allowing for the realization of two-dimensional ferromagnetism. Spin fluctuations at fixed temperature can, however, be enhanced in low-dimensional ferromagnets. There have been numerous investigations into the coupling of the magnetic moment with the conduction electrons and the resulting magnetoresistive phenomena [2,3], but little focus on the intrinsic contribution of magnetic scattering due to spin waves that result from electron-magnon scattering events and s - d interaction. This is of importance in the high magnetic field regime [4]. In particular, there is no experimental investigation into the interfacial modification of electron-magnon spin-flip scattering as the thickness of a thin film is reduced—something that is of particular importance with regard to the spin coherence length critical to spintronic devices [5].

Anisotropic magnetoresistance (AMR) is a direct consequence of s - d scattering in ferromagnets and is very sensitive to the distribution of the density of states at the Fermi energy [6], taking on a negative value for half metals [7]. AMR was explained by Smit [8] by the introduction of the spin-orbit interaction (SOI) through a perturbation that is suggested to result in an unequal distribution of d states, such that there exists more orbitals parallel to the magnetization rather than perpendicular to it, resulting in a shorter and longer mean-free path, respectively. This analysis was performed within the Mott two-current model [9] where s - d scattering makes the greatest contribution to the resistivity. The SOI, responsible for AMR, is of great interest due to its involvement in such phenomena as the spin Hall effect [10], the Dzyaloshinskii-Moriya interaction [11,12], and precessional damping [13,14].

The AMR ratio is defined as

$$\frac{\Delta\rho}{\rho} = \frac{\rho_{\parallel} - \rho_{\perp}}{\rho_{\perp}}, \quad (1)$$

where $\Delta\rho$ is the difference between resistivities for current parallel (ρ_{\parallel}) and transverse (ρ_{\perp}) to the orientation of the magnetic field. For thin films it is well known that the AMR ratio decreases with reducing film thickness [15], which has been attributed to an increasing sample resistivity due to the size effect [16] while $\Delta\rho$ remains constant [15]. However, contrary to this description it has been found that $\Delta\rho$ also decays with reducing film thickness [17,18]. To date the reason for this thickness dependence of AMR has not been clear, but in this paper we present a coherent physical explanation for this phenomenon, supported by experimental evidence for the underlying mechanism.

The theory of Smit was successful in explaining AMR but made few quantitative predictions. Campbell and Fert, however, explained temperature dependent deviation of the resistivity of ferromagnet-based alloys from Matthiessen's rule in terms of the two-current model [19], and later with Jaoul expanded this into a quantitative theory for the AMR ratio in Ni-based alloys [20]. Using a Boltzmann analysis within the two-current model they arrived at the equation

$$\frac{\Delta\rho}{\rho} = \frac{\gamma(\rho_{\downarrow} - \rho_{\uparrow})\rho_{\downarrow}}{\rho_{\uparrow}\rho_{\downarrow} + \rho_{\uparrow\downarrow}(\rho_{\uparrow} + \rho_{\downarrow})}, \quad (2)$$

which successfully described the AMR in lightly doped Ni alloys. The constant γ (≈ 0.0075) [20] is proportional to the strength of the SOI energy relative to the exchange energy. The terms ρ_{\uparrow} and ρ_{\downarrow} parametrize the resistivity of the two spin conduction channels within the Mott two-current model. The term $\rho_{\uparrow\downarrow}$ parametrizes spin mixing arising from the coupled Boltzmann equations, one for each conduction channel. This spin mixing can be attributed to electron-magnon scattering [20]. This theory showed that the AMR ratio was largest for alloys with the largest $\rho_{\downarrow}/\rho_{\uparrow}$, which depends on the density of states at the Fermi energy which can be manipulated using dopants.

In this paper experimental results and analysis of AMR in doped Ni thin films as a function of thickness are presented. A rapid decrease of the AMR ratio and $\Delta\rho$ was observed as the film thickness was reduced below 6 nm. It is hypothesised from this that the loss of AMR is a consequence of enhanced electron-magnon spin-flip scattering in the thinnest films.

*del.atkinson@durham.ac.uk

Good agreement was observed between the AMR ratio data as a function of thickness and a modified Campbell, Fert, and Jaoul (CFJ) theory where we have incorporated thickness dependence into the $\rho_{\uparrow\downarrow}$ spin-mixing term. From temperature dependent magnetization measurements the spin-wave stiffness was determined as a function of sample thickness and shown to decrease with sample thickness, consistent with the thickness at which the fall in $\Delta\rho$ is observed. The reduced spin-wave stiffness in the thinnest films leads to enhanced spin mixing such that the conduction channels for the spin- \uparrow and spin- \downarrow electrons can no longer be treated independently, leading to the breakdown of the Mott two-current model and the observed fall in $\Delta\rho$.

II. EXPERIMENT AND RESULTS

Samples were prepared by sputter deposition onto Si substrates with ~ 100 nm thermally grown oxide coating with base pressures of the order 10^{-8} Torr. Deposition was performed through a $18\text{ mm} \times 3\text{ mm}$ mask to create a well defined geometry for the resistivity measurements. Ni was doped with Cr and V by cosputtering and the deposition rates were adjusted to obtain the required dopant concentration, which was set at 5% for both dopants. X-ray reflectivity (XRR), magneto-optical Kerr effect, transmission electron microscopy (TEM), and superconducting quantum interference device-vibrating sample magnetometry (SQUID-VSM) was used to characterize the samples. XRR of the thickest samples showed that prolonged exposure to atmosphere resulted in the formation of an ~ 1 nm oxide layer on the surface of the samples with a root-mean-square roughness of order 0.5 nm. This oxide is highly electrically resistive, meaning there was no need for current shunting corrections in the AMR analysis, which would be required if metallic capping layers had been used.

AMR was measured using a standard four-probe technique. The sample was rotated through 180° in a saturating in-plane magnetic field and the resulting distribution of resistivities was fitted with

$$\rho = \rho_{\perp} + \Delta\rho \cos^2(\theta + \theta_c), \quad (3)$$

to extract the AMR, where θ is the angle between the magnetic field and the current and θ_c is a small constant correction angle (typically $\sim 2^\circ$) required due to offsets in the sample alignment with respect to the magnetic field. Figure 1 shows some examples of the angular dependence of the resistivity fitted with the above equation for different thicknesses of Ni.

Magnetoresistance measurements were taken for pure and doped Ni films as a function of film thickness. The inset for Fig. 2 shows the thickness dependence of $\Delta\rho$ for pure and doped Ni samples. Above 6 nm $\Delta\rho$ rises gradually, approaching a constant bulk value consistent with Potter and McGuire [15] whose earlier work indicated no dependence of $\Delta\rho$ on the film thickness. This bulk value of $\Delta\rho$ is dependent on the dopant species and scales in accordance with the predictions of CFJ [20]. The smallest AMR occurs for Cr doped samples due to the formation of a d_{\uparrow} bound state close to the Fermi energy [21] increasing the value of ρ_{\uparrow} . Following normalization with respect to the saturated $\Delta\rho$ value for each dopant it can be seen in the main figure that all the data

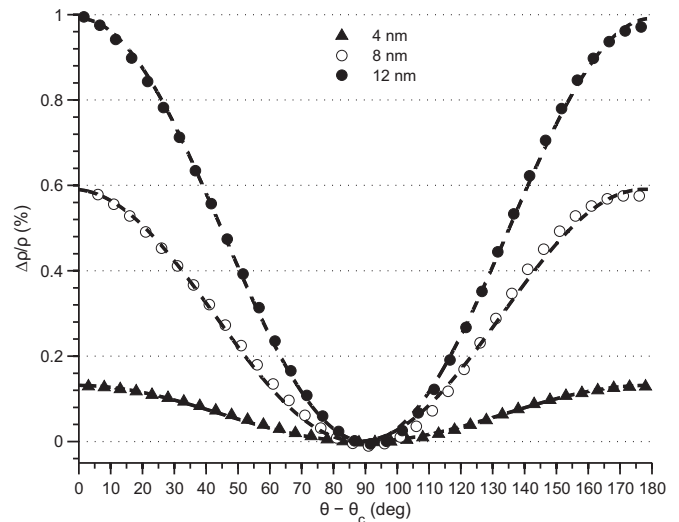


FIG. 1. The dependence of the resistivity on the angle between the magnetic field and applied current plotted as the percentage AMR ratio for different thicknesses of Ni films. The lines are best fits made using Eq. (3) from which $\Delta\rho$ and ρ_{\perp} were extracted. It can be seen that the AMR ratio reduces as a function of thickness.

points fall onto the same curve, irrespective of dopant. This universal scaling suggests that the loss of $\Delta\rho$ is due entirely to the effect of the reduced dimensionality of the sample, independent of the material details involved. It can be seen in Fig. 3 that the thickness at which $\Delta\rho$ begins to fall coincides well with the thickness at which the resistivity diverges, which is known to be largely interface driven [16]. The linear fits in the inset of Fig. 3, where $\Delta\rho$ is plotted against ρ_{\perp} demonstrate the interdependence of the two variables. This loss of $\Delta\rho$ is not due to the rise in sample resistivity but instead both these

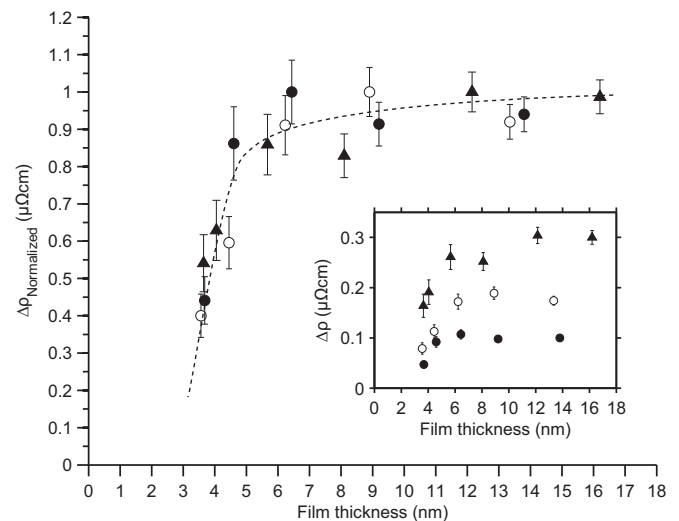


FIG. 2. Inset: $\Delta\rho$ as a function of film thickness for Ni (triangles), Ni:V (open circles), and Ni:Cr (filled circles). The rapid drop in $\Delta\rho$ occurs for films below 6 nm irrespective of the dopant. This is shown clearly by the main figure in which $\Delta\rho_{\text{Normalized}}$ (with respect to the saturation value of each alloy) is plotted against film thickness. This is strong evidence that the loss of $\Delta\rho$ is interface driven.

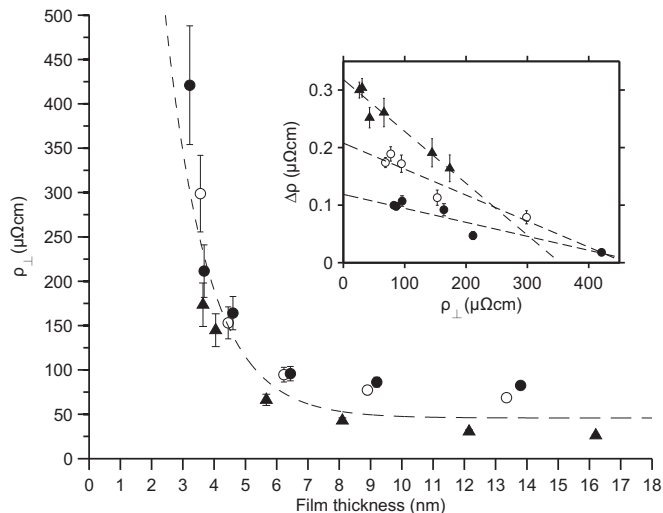


FIG. 3. Sample resistivity (ρ_{\perp}) for Ni (triangles), Ni:V (open circles), and Ni:Cr (filled circles) as a function of film thickness. The rapid rise in ρ_{\perp} in the thinnest films is known to be due to enhanced scattering from the sample interfaces. The dashed line is a fitted exponential. The inset shows $\Delta\rho$ plotted against the sample resistivity. The two scale linearly with each other providing evidence that $\Delta\rho$ like ρ_{\perp} is modified by the reduced dimensionality.

parameters are modified by the same effect, the increasing contributions of the interfaces and reduced dimensionality of the sample. This is contrary to the theoretical work of Dieny *et al.* [22] who predicted an enhanced $\Delta\rho$ in the thin film limit when contributions from nonspecular, spin-conserving scattering from interfaces becomes dominant.

We turn now to the microscopic origin of this loss of AMR. Referring to Eq. (2) we can interpret phenomenologically how reducing the sample thickness will modify each variable. The spin channel resistivities ρ_{\uparrow} and ρ_{\downarrow} are related primarily to the density of states of the system. Although it is known that the density of states is modified by sample thickness, this is not significant until the ultrathin regime where the thickness is of the order of monolayers [23]. The parameter γ would be little modified on the length scales in this investigation as the exchange and spin-orbit interactions are atomic in origin. Interestingly the exchange length of Ni (≈ 8.3 nm) [24] coincides with the thickness at which $\Delta\rho$ begins to fall. Reducing the sample thickness below the exchange length would have consequences for the spin-wave stiffness and the magnon density of states. A detailed theoretical analysis of the contribution of spin-flip scattering in ferromagnetic films has been undertaken within a Boltzmann framework by Ren and Dow [25] and showed significantly enhanced spin-flip scattering for thin films on the nanometer scale. This suggests the loss of the AMR is due to the enhancement of the $\rho_{\uparrow\downarrow}$ in thin films.

Therefore, we have incorporated the thickness dependence into the $\rho_{\uparrow\downarrow}$ term in Eq. (2). Since this term contributes to the overall resistivity (by introducing mixing between the two spin channels) this term is given the same functional thickness dependence as the measured sample resistivity.

The resistivity data in Fig. 3 was fitted with both Mayadas-Shatzes [26] and Fuchs-Sondheimer [16] models. Both gave

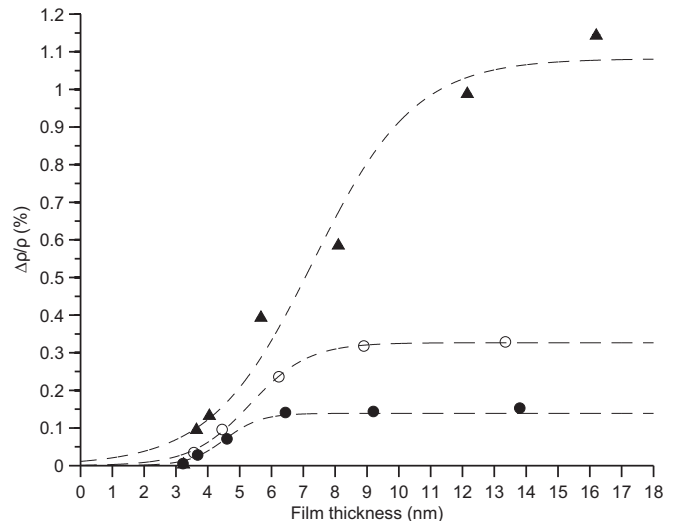


FIG. 4. The measured percentage AMR ratios for Ni (triangles), Ni:V (open circles), and Ni:Cr (filled circles) as a function of film thickness. The drop in AMR is associated with the combined action of increasing sample resistivity as well as vanishing $\Delta\rho$. The lines are best fits of Eq. (2) with thickness dependence incorporated into the $\rho_{\uparrow\downarrow}$ using Eq. (4).

good agreement for the thicker films but failed for the thinnest samples. TEM analysis on 15, 6, and 4 nm Ni films deposited on silicon nitride windows showed that this failure is due to the presence of voids between clusters of columnar grains for films thinner than 6 nm. An exponential, however, captures the form of the resistivity data well, as is demonstrated in Fig. 3. The same empirical functional form for the thickness dependence has thus been applied to $\rho_{\uparrow\downarrow}$ using

$$\rho_{\uparrow\downarrow}(t) = \rho_{\uparrow\downarrow,\text{bulk}} + \rho_{\uparrow\downarrow}(0) \exp(-t/t_0), \quad (4)$$

where $\rho_{\uparrow\downarrow,\text{bulk}}$ corresponds to the spin-mixing resistivity for the bulk material, $\rho_{\uparrow\downarrow}(0)$ is a hypothetical zero-thickness spin-mixing resistivity, and t_0 is the critical thickness which scales the exponential. This functional form is in good qualitative agreement with that predicted by Ren and Dow [25] for the thickness dependence of the spin-mixing resistivity.

A plot of the AMR ratio as a function of thickness can be seen in Fig. 4 with fits using Eq. (2) and thickness dependence incorporated by substituting Eq. (4) for $\rho_{\uparrow\downarrow}$. It can be seen that this simple model fits the data very well. The values for the parameters extracted from the fits are shown in Table I. The ratio of ρ_{\uparrow} and ρ_{\downarrow} can be seen to approach unity with the separate dopants, consistent with the expected modification to the density of states brought about by the impurities. Note also

TABLE I. Best-fit parameters found from fitting Eq. (2) with thickness dependence incorporated using Eq. (4) to the $\Delta\rho/\rho$ data in Fig. 4.

	$\rho_{\downarrow}(\mu\Omega \text{ cm})$	$\rho_{\uparrow}(\mu\Omega \text{ cm})$	$\rho_{\downarrow}/\rho_{\uparrow}$	$\rho_{\uparrow\downarrow,\text{bulk}}(\mu\Omega \text{ cm})$
Ni	300	116	2.6	8.5
Ni:V	222	126	1.8	60.1
Ni:Cr	193	131	1.5	119.9

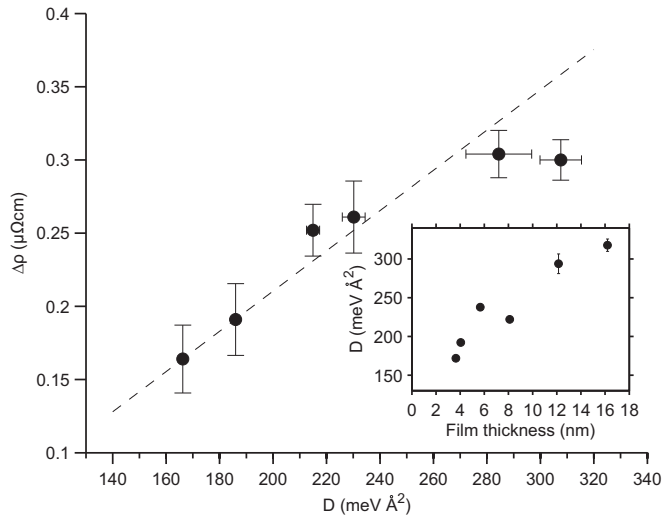


FIG. 5. Inset: Spin-wave stiffness (D) as a function of Ni film thickness. The rapid drop in D coincides well with the drop in $\Delta\rho$, suggesting that the loss of AMR is due to enhanced electron-magnon spin-flip scattering. The main figure shows $\Delta\rho$ plotted against D . A linear fit has been made to the data which supports the correlation, demonstrating that the reduction in $\Delta\rho$ is a consequence of the reduced spin-wave stiffness in thin films.

that the bulk material value of $\rho_{\uparrow\downarrow}$ also shows a dependence upon the species of impurity.

The enhancement of $\rho_{\uparrow\downarrow}$ in thin films suggests an increased number of thermally activated magnons. To support this, magnetization as a function of temperature measurements were obtained using a SQUID-VSM for the pure Ni samples so that the spin-wave stiffness D could be derived. The spin-wave stiffness is given by the curvature of the magnon dispersion relation at zero wave vector [27] and is representative of the energy required to create a short wave-vector magnon excitation. Fitting the data with a Bloch 3/2 law allows the β parameter as well as $M(0)$, the magnetization at zero Kelvin, to be extracted.

From these experimentally determined parameters, the spin-wave stiffness can be obtained from [28]

$$D = \frac{k_B}{4\pi} \left(\frac{\zeta(3/2)g\mu_B}{M(0)\beta} \right)^{2/3}, \quad (5)$$

where k_B is the Boltzmann constant, $\zeta(3/2) = 2.612$ is the Riemann zeta function, $g = 2.20$ [29] is the g factor, and μ_B is the Bohr magneton. In the inset of Fig. 5 the extracted values of D are plotted as a function of Ni thickness. It can be seen that D falls as the thickness decreases. There is also an indication that for thicknesses below 6 nm D drops more rapidly. This drop is likely associated with the onset of discontinuities in the film resulting in an increased surface contribution with high spin disorder and consequently reduced spin-wave stiffness. This has been observed in clusters of Ni nanoparticles [30]. In Fig. 5 a plot of $\Delta\rho$ against D is shown. The linear dependence between the two variables confirms that the loss of $\Delta\rho$ is associated with a reduction of spin-wave stiffness.

III. CONCLUSIONS

In this paper it is shown that the AMR ratio falls due to the combined effect of increasing sample resistivity as well as a previously unexplained fall of $\Delta\rho$ as sample thickness is reduced. This loss of $\Delta\rho$ is rapid below 6 nm. Good agreement between experiment and a simple model were found when sample thickness was incorporated into the CFJ theory through the spin-mixing resistivity which encompasses spin-flip scattering mechanisms. Further evidence supporting electron-magnon spin-flip scattering was found from SQUID-VSM measurements from which the spin-wave stiffness was derived. Plotting spin-wave stiffness as a function of Ni film thickness yielded a dependence that, like $\Delta\rho$, showed a drop-off for thicknesses below 6 nm. Indeed $\Delta\rho$ scales linearly with the spin-wave stiffness. It is expected that a reduction would result in enhanced electron-magnon scattering and consequently enhanced spin-flip scattering. This leads to the eventual breakdown of the Mott two-current model in thin films since the conduction channel for each spin can no longer be treated as independent.

ACKNOWLEDGMENTS

This work was funded by The Engineering and Physical Sciences Research Council (EPSRC), the Royal Society, and Durham University. R.M.R.-R. gratefully acknowledges a DTA studentship award. The authors are grateful to O. Cespedes for assistance and access to the EPSRC SQUID-VSM facility at the University of Leeds as well as B. Mendis for the TEM measurements at Durham University.

-
- [1] N. D. Mermin and H. Wagner, *Phys. Rev. Lett.* **17**, 1307 (1966).
 - [2] S. S. P. Parkin, *Annu. Rev. Mater. Sci.* **25**, 357 (1995).
 - [3] S. Yuasa and D. D. Djayaprawira, *J. Phys. D* **40**, R337 (2007).
 - [4] B. Raquet, M. Viret, E. Sondergard, O. Cespedes, and R. Mamy, *Phys. Rev. B* **66**, 024433 (2002).
 - [5] G. Balasubramanian, P. Neumann, D. Twitchen, M. Markham, R. Kolesov, N. Mizuochi, J. Isoya, J. Achard, J. Beck, J. Tissler *et al.*, *Nat. Mater.* **8**, 383 (2009).
 - [6] S. Kokado, M. Tsunoda, K. Harigaya, and A. Sakuma, *J. Phys. Soc. Jpn.* **81**, 024705 (2012).
 - [7] F. J. Yang, Y. Sakuraba, S. Kokado, Y. Kota, A. Sakuma, and K. Takahashi, *Phys. Rev. B* **86**, 020409 (2012).
 - [8] J. Smit, *Physica* **17**, 612 (1951).
 - [9] N. F. Mott, *Proc. R. Soc. London, Ser. A* **153**, 699 (1936).
 - [10] J. E. Hirsch, *Phys. Rev. Lett.* **83**, 1834 (1999).
 - [11] I. Dzyaloshinsky, *J. Phys. Chem. Solids* **4**, 241 (1958).
 - [12] T. Moriya, *Phys. Rev.* **120**, 91 (1960).
 - [13] T. Gilbert, *IEEE Trans. Magn.* **40**, 3443 (2004).
 - [14] Y. Tserkovnyak, A. Brataas, and G. E. W. Bauer, *Phys. Rev. Lett.* **88**, 117601 (2002).
 - [15] T. McGuire and R. Potter, *IEEE Trans. Magn.* **11**, 1018 (1975).
 - [16] E. Sondheimer, *Adv. Phys.* **1**, 1 (1952).
 - [17] N. T. Thanh, L. T. Tu, N. D. Ha, C. O. Kim, C. Kim, K. H. Shin, and B. Parvatheeswara Rao, *J. Appl. Phys.* **101**, 053702 (2007).

- [18] L. K. Bogart, Ph.D. thesis, Durham University, 2010, <http://etheses.dur.ac.uk/507/>.
- [19] A. Fert and I. A. Campbell, *Phys. Rev. Lett.* **21**, 1190 (1968).
- [20] I. A. Campbell, A. Fert, and O. Jaoul, *J. Phys. C* **3**, S95 (1970).
- [21] J. Friedel, *Nuovo Cimento* **7**, 287 (1958).
- [22] B. Dieny, M. Li, S. H. Liao, C. Horng, and K. Ju, *J. Appl. Phys.* **88**, 4140 (2000).
- [23] M. Hoesch, V. N. Petrov, M. Muntwiler, M. Hengsberger, J. L. Checa, T. Greber, and J. Osterwalder, *Phys. Rev. B* **79**, 155404 (2009).
- [24] G. S. Abo, Y. Hong, J. Park, J. Lee, W. Lee, and B. Choi, *IEEE Trans. Magn.* **49**, 4937 (2013).
- [25] S. Y. Ren and J. D. Dow, *Phys. Rev. B* **61**, 6934 (2000).
- [26] A. F. Mayadas and M. Shatzkes, *Phys. Rev. B* **1**, 1382 (1970).
- [27] M. Pajda, J. Kudrnovsky, I. Turek, V. Drchal, and P. Bruno, *Phys. Rev. B* **64**, 174402 (2001).
- [28] J. W. Lynn and J. J. Rhyne, *Spin Waves and Magnetic Excitations* (North-Holland, Amsterdam, 1988).
- [29] N. Bloembergen, *Phys. Rev.* **78**, 572 (1950).
- [30] S. Vitta, *J. Appl. Phys.* **101**, 063901 (2007).